Miranda Waldman

Capstone Final Paper

Shooting Range Remediation: Using kriging to delineate the extent of lead contamination in soil from an uneven sample pattern

Abstract

Shooting ranges are a source of large lead accumulations, contributing to rising lead levels in soil. This study examines measured lead levels in soil samples taken from a shooting range in Pennsylvania, with the goal of producing a continuous surface identifying areas exceeding the Pennsylvania Department of Environmental Protection limit of 450 parts per million per the Statewide Health Standard for Medium Specific Concentrations of Inorganic Regulated Substances: Soil-to-Groundwater Values. Several data challenges impacted the spatial interpolation of the measured lead levels, including an uneven sampling pattern used to obtain the soil samples and an extremely skewed distribution. Several kriging methods were applied to delineate the extent of lead contamination with the goal of minimizing estimation error. In addition, several study area delineations were compared to address the uneven sampling scheme. The study found that indicator kriging in general was able to handle the skewed distribution and produce a lead level surface with acceptable estimation areas.

Introduction

Background

For decades, lead levels in soil have been increasing due to human activity (US EPA, 2020). This is a growing concern as the health effects of high lead levels are numerous, affecting almost every organ and system in the human body (ATSDR 2020). Lead does not break down, so when it gets into the soil it stays there (US EPA, 2020; ATSDR, 2020). Lead in soil can impact humans in a variety of ways, including: 1) fruits and vegetables that are grown in contaminated soil can create toxic food and, 2) playing or touching bare contaminated soil can lead to exposure, which is a common source of exposure for children (USA EPA, 2020).

Shooting ranges are recognized for being a source of large lead accumulations in the environment. Studies on the concentrations of lead at shooting ranges have found values as high as 10,000 to 70,000 mg/kg in soil (Sanderson et al., 2018). This is in comparison to the natural levels of lead in soil, which can range from 50 to 400 mg/kg (US EPA, 2015). Up until 1993, there was very little regulation on shooting ranges from the federal government. That changed when a U.S. Court of Appeals ruled that soil contaminated by lead shot could be considered hazardous waste if unclaimed (Hardison et al., 2003). Because of this most shooting ranges have adopted lead management plans, which include many ways to prevent lead from getting into or migrating within soil (US EPA, 2005). But in cases where lead is present in the soil, it is necessary to treat it to prevent further spread.

One way lead contaminated soil is treated is through environmental remediation, which involves removing or minimizing the lead hazard (Dobrescu et al., 2022). This is often very expensive, and the costs can increase drastically at large sites, especially if the scope of work changes throughout a project (Dahlem, 2021). Because of this it is crucial to characterize or estimate the extent of lead contamination as accurately as possible. Characterization of a site typically involves taking samples and submitting them to laboratories to determine the level of the contaminant of concern at that sample location (Anderson Engineering, 2021). These samples represent points for an area of interest and are not a continuous representation of contamination on a site. To assist in characterization, interpolation methods are often utilized.

Spatial interpolation estimates the value of a variable at an unknown point based on the values of the variable measured at a limited set of known points. There are many spatial interpolation methods to choose from, and each has different strengths and use cases. Kriging is a common approach used in soil, geology, and environmental science applications (GISGeography, 2022). Kriging is a stochastic method of interpolation, which differs from commonly used deterministic methods like IDW and Nearest Neighbor interpolation. Deterministic methods assume that the data points being input are exact and use a deterministic mathematical equation to carry out the interpolation (O'Sullivan and Unwin, 2010). This means that the combination of the data, methods, and required parameters are uniquely determined. The chosen parameters can be argued, but otherwise the results are able to be verified and repeated. O'Sullivan and Unwin argue that deterministic methods are unrealistic for two reasons. First, no environmental measurements can be made without error as data is often a snapshot in time of a pattern. And second, parameters used in deterministic interpolators generalize phenomena and make an assumption about the spatial behavior of the characteristic of interest. Stochastic methods, on the other hand, recognize our lack of knowledge regarding the spatial variation of the phenomena of interest and allow for uncertainty in the estimation process. Stochastic methods, like kriging, make use of the spatial variability present in the sample data to better inform the interpolation approach. Stochastic methods introduce random elements into the interpolation process, resulting in multiple possible interpolated surfaces for the same set of data and parameters. More importantly the statistical significance and error of a surface can be calculated (GIS Resources, 2013).

Kriging is a multi-step process. The first step in kriging is creating a variogram with the sample data to describe the variability of data across space (O'Sullivan and Unwin, 2010). The variogram describes the spatial dependence in the variable of interest and plots semivariance as a function of distance. Semivariance captures the degree of dissimilarity in the value of the points separated by a defined distance and the shape describes the degree of spatial autocorrelation present in the variable. Second, a mathematical model is fit to the observed semivariogram that best approximates the observed spatial dependence and allows for the prediction of semivariance values at all distances. This model is then used to determine the interpolation weights. The result is an interpolated surface and the means to calculate an estimation variance, which can be mapped to estimate the error.

There are many different forms of kriging, reflecting differences in the assumptions made with regards to the underlying surface. And multiple kriging approaches have been used to interpolate lead in soil. Alexander (2016) used block kriging to determine the extent of lead at concentrations of 400 mg/kg. In this case, each block contained an estimated range of values which summarized the average sample values within the block. This method was chosen because of previous experience in applying kriging to developing excavation plans for contaminated soil. The 30 by 30-foot blocks in their analysis corresponded to blocks that were excavated in the field. Francos et al. (2022) examined the distribution of lead in soil in a contaminated area using a Getis-Ord hotspot analysis and then employed simple kriging on the z-score values resulting from the hotspot analysis. They chose simple kriging as the z-scores at each location were drawn from a normal distribution, which assumes that the mean is 0 across the study area. They found that using interpolation on their data predicted values with a high level of certainty. They also found that topography may play a role in how values are distributed, although they did not include a measure of elevation in their kriging analysis. Miryousefiaval et al. (2020) used ordinary kriging to interpolate lead values and compared the resulting interpolated surface to an interpolated surface derived from satellite imagery. They investigated several possible variogram models, for example Gaussian and spherical. They also used cross-validation and multiple error statistics, for example MAE and RMSE, to select the best model and produce their final interpolated surface. It can be seen from these three examples that kriging is often utilized for determining the extent of lead in soil, but that there is not a one size fits all method for all cases.

Nonparametric kriging approaches have also been utilized to delineate lead in soil and in groundwater. Nonparametric approaches allow skewed or unevenly distributed data to be used for an estimation without interference because of these variations (Juang and Lee, 2000). Two examples of nonparametric approaches are indicator kriging and probability kriging. Indicator kriging takes the values of the input dataset and creates a binary value using a threshold. These binary values are then interpolated which produces a surface that indicates the probability of exceeding the defined threshold. The challenge of this model is that there is a loss of information when transforming the data to binary values. Probability kriging also uses binary values based on a defined threshold, but it also includes a secondary variable. This secondary variable is the original values, which inform the binary data, also making this method a form of cokriging (de Smith et al., 2021). This method is more complicated than indicator kriging as it requires that a variogram is fit to the binary data, original data, and the cross-correlation values. This brings in more uncertainty and estimation into the interpolation (Esri, n.d.). Juang and Lee compared three nonparametric kriging methods to determine which performed best at delineating heavy metals, including lead, in soil. They examined indicator kriging, probability kriging, and kriging with the cumulative distribution function (CDF) of order statistics (CDF kriging). They found that CDF kriging and probability kriging were more accurate than indicator kriging. Adhikary et. al. (2010) looked at indicator and probability kriging, but for heavy metals in groundwater. They found that probability kriging performed better than indicator as well, suggesting that incorporating order relations information improved estimations.

Often sample data are not distributed evenly across a site location. This uneven sampling distribution can influence which kriging or interpolation method is chosen. Brus and Heuvelink (2007) attempted to create an optimal configuration of sampling locations for finding the mean highest water table across a site for universal kriging by attempting to minimize the variances in universal kriging. In their case study they found that optimizing the sampling locations made a considerable difference in the results. Another consideration is that the spatial structure of the variable itself may vary across the area of intereset. Liu et al. (2021) studied stratified ordinary kriging on data with heterogeneity in land use types. They classified their site into four areas, and considered for each strata how the soil and land types were related to soil carbon, their variable of interest. Breaking their study area allowed them to capture soil carbon through a secondary variable and then run an individual variogram model for each strata. The assumption in using stratified ordinary kriging is that the strata are uniform in their properties, so there needs to be high variability between strata, but low variability between the attribute value within the strata. It is worth considering when carving a site into pieces what the best way is to classify various sampling points.

Goals and Objectives

In the case of environmental remediation, the extent of contamination needs to be defined. Kriging has been utilized in many studies as a method of delineating lead in soil and interpolating samples that have not been taken in an even pattern. This study will utilize spatial interpolation to determine locations within the shooting range and in the immediate adjacent areas that have lead levels over the Pennsylvania Department of Environmental Protection's (PA DEP) Statewide Health Standard for Medium Specific Concentrations of Inorganic Regulated Substances for the Soil-to-Groundwater Values. This value is 450 mg/kg (2021). This study will employ several kriging methods and strategies to address the uneven nature of the sampled data to determine which approach is the most suitable based on the minimization of error.

Methodology

Study Area

The study area is a shooting range located in southwestern Pennsylvania. Currently this shooting range serves as a sporting clay course, which is compared to playing golf with a shotgun (NSCA, n.d.) These shotguns typically contain a shot with hundreds of tiny lead balls, which disperse in the air to create multiple projectiles (Adventure Sports, n.d.). The study area encompasses the shooting range property and the immediate surrounding areas, which is approximately 275 acres in size. The exact location of this site must remain anonymous. The data has been provided from this author's place of employment, an environmental consulting firm. A condition of using this data is that the client's name and location must be kept private.

Data

The main dataset used for this analysis is a set of 442 point features representing soil sample locations (Figure 1). Most of the samples were collected in a 100-foot grid pattern, but several samples did not follow this pattern especially within the shooting range property. Onsite, there are many gaps in the sampling distribution, resulting in large gaps in the data. This was done because the property owner is less interested in the remediation of their own property, focused instead on the offsite properties they contaminated. Each sample was collected between 0 and 6 inches below the ground surface using a disposable sampling trowel. Samples were then homogenized to create a representative sample with the goal of achieving a consistent physical appearance and texture and to evenly distribute the geochemical characteristics of the soil over the entire sample. This is done to eliminate or minimize analytical bias prior to transferring the soil into laboratory provided sample jars. The samples were collected between 2019 and 2022.

As mentioned in the previous section, the location of the data must be kept private. Because of this, all maps made for this analysis will be made without a basemap, and at the end of the analysis all data will be moved to another location on the map as an extra layer of privacy. In addition, any reference in the data that could tie it back to the property owner will be removed like the names given to each sample.

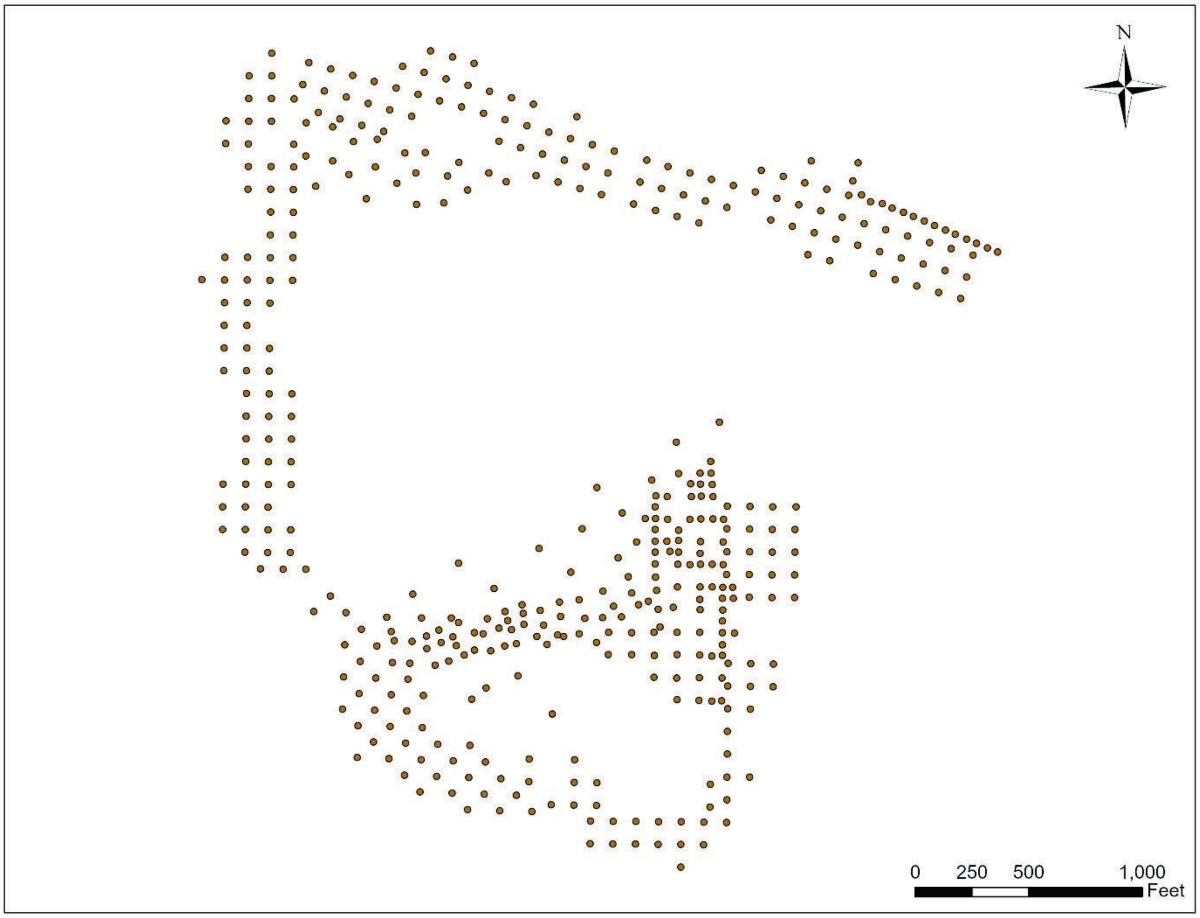

Figure 1: Soil sample locations within the study area.

Statistical Analysis

An exploratory analysis was completed to ensure that this dataset was suitable for the kriging methodology outlined above. First, a histogram was made with the lead values, to determine the distribution of the data (Figure 2). It was evident that lead values did not follow a normal distribution, with noticeable positive skewing and several samples displaying extremely high lead values, with outliers above 70,000-pmm, an already high value found at shooting ranges. Distributions marked by positive skewing are a common occurrence in environmental data, and often follow a log distribution given measure environmental data is bounded at 0 (Griffith, 2002). Because of this, the sampled lead levels were natural log transformed to better approximate a normal distribution. The resulting histogram was less skewed and better approximated a normal curve (Figure 3), although the data transformation did not completely remove positive skewing in the data.

Global Moran's I was calculated for the original measured lead levels to determine the presence and significance of spatial autocorrelation in the soil samples. Neighbors were defined as all points within a 150 feet radius of each sampled location. This was chosen because the majority of the sample locations were collected on a 100-foot grid. The value of 150 ft encompasses the diagonal distances between these sample locations. The calculated Moran's I value was 0.147343 ($p \approx 0$), which indicates significant positive spatial autocorrelation in lead values for the dataset. The confirmation of spatial structure in the sample points confirmed the suitability of employing a spatial interpolation approach.

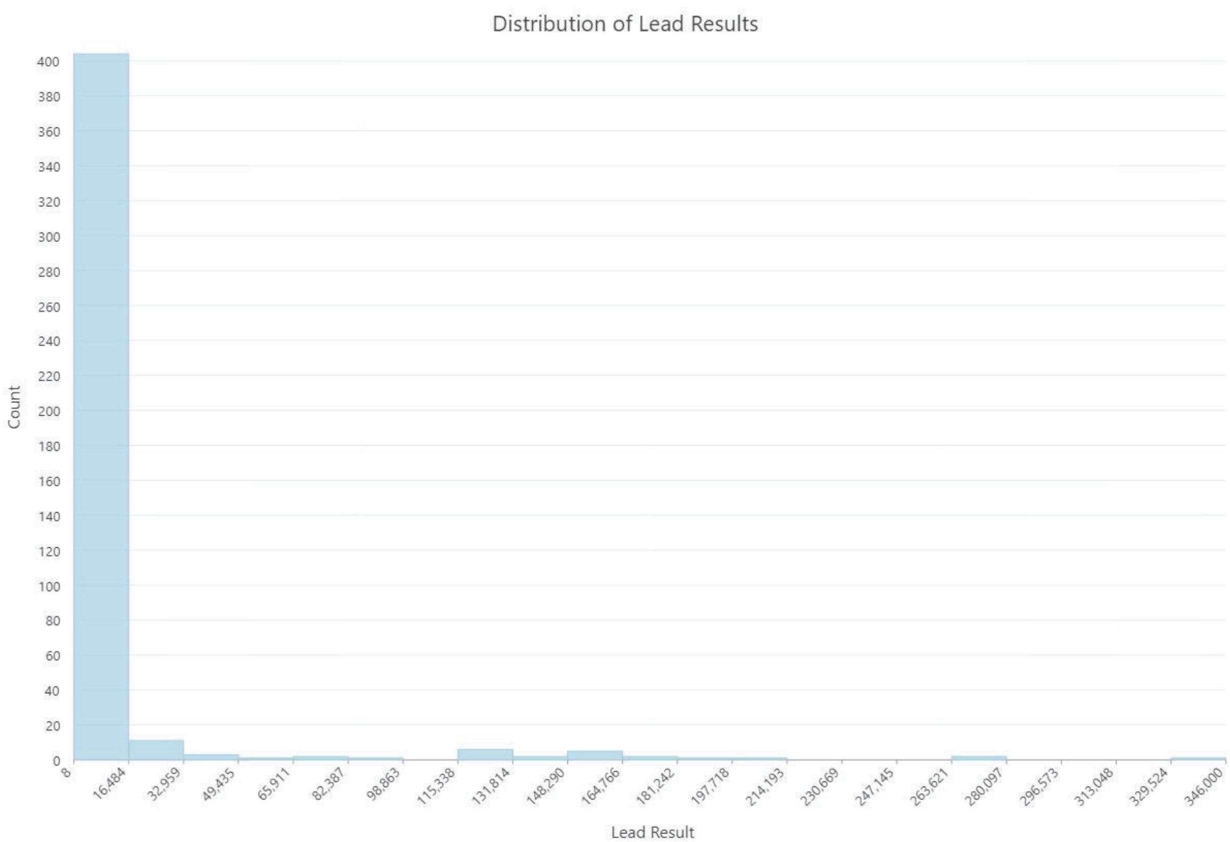

Figure 2: Distribution of the soil sample lead values.

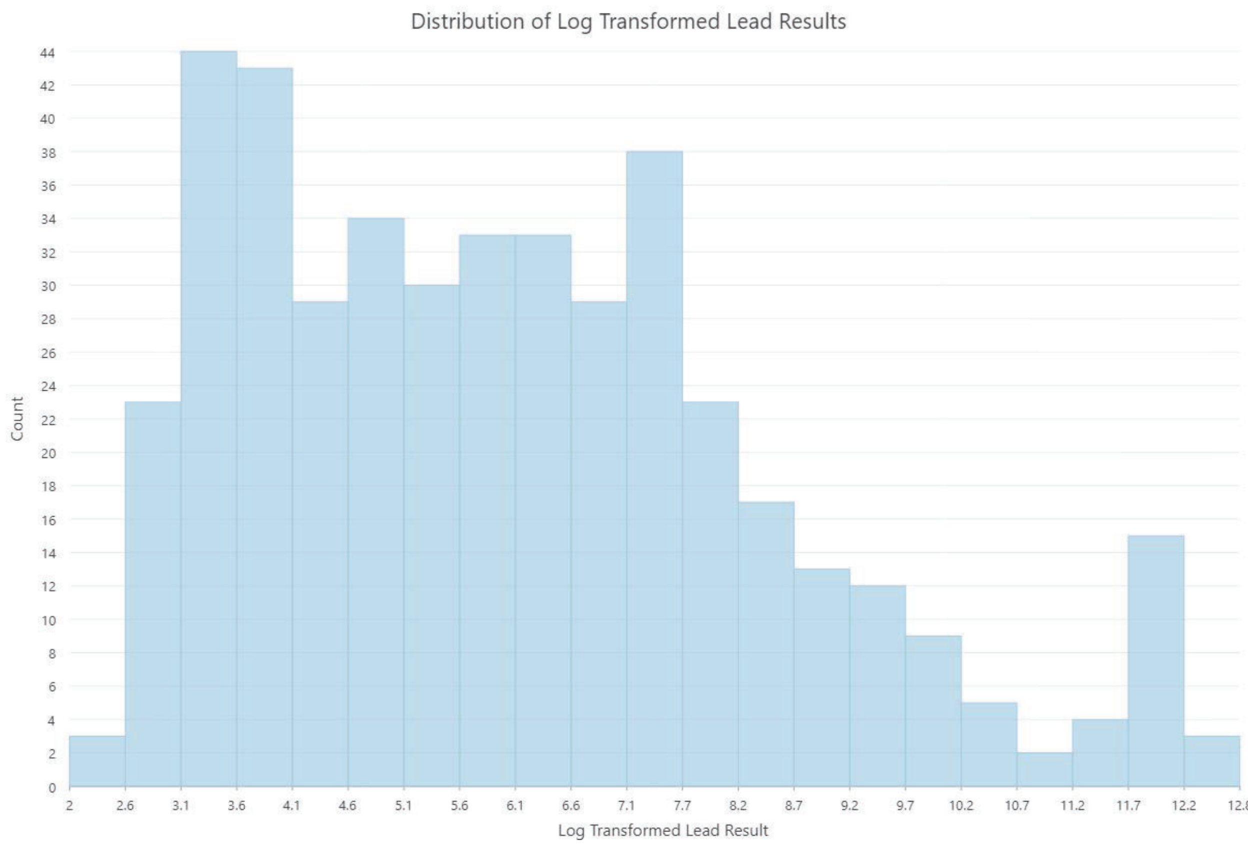

Figure 3: Distribution of the log-transformed lead values.

Methods/Analysis

This study utilized kriging to determine the boundary of the lead clean up area. Two kriging models were examined – indicator kriging and probability kriging. Indicator kriging works by taking a threshold or cutoff value and coding the data into zeros and ones based on that threshold (Goovaerts, 1997). The equation for this transformation is as follows, with the threshold value defined as z_k and the value of a specific location defined as u_α:

$$i(\mathbf{u}_\alpha; z_k) = \begin{cases} 1 & \text{if } z(\mathbf{u}_\alpha) \leq z_k \\ 0 & \text{otherwise} \end{cases}$$

The estimator for indicator kriging, which estimates a local indicator mean at each sampled location based on the defined neighborhood, is defined as follows:

$$[I(\mathbf{u}; z_k)]^* - \mathrm{E}\{I(\mathbf{u}; z_k)\} = \sum_{\alpha=1}^{n(\mathbf{u})} \lambda_\alpha(\mathbf{u}; z_k)\ [I(\mathbf{u}_\alpha; z_k) - \mathrm{E}\{I(\mathbf{u}_\alpha; z_k)\}]$$

It should be noted that indicator kriging is an exact estimator, meaning it honors the indicator value at sampled locations (Goovaerts, 1997). Indicator kriging produces a surface that estimates the probability of a location being above or below the designated cutoff value.

Probability kriging, a variant of indicator kriging, also transforms the data using an indicator transformation. However, probability kriging also takes into account the original measured values in an attempt to preserve the information lost when transforming the data to an indicator variable. Probability kriging can be thought of as a form of indicator co-kriging. The probability kriging estimator is defined as follows:

$$\begin{aligned}[F(\mathbf{u}; z_k|(n))]^*_{PK} &= [I(\mathbf{u}; z_k)]^*_{PK} \\ &= \sum_{\alpha=1}^{n(\mathbf{u})} \lambda_\alpha^{PK}(\mathbf{u}; z_k)\, I(\mathbf{u}_\alpha; z_k) + \sum_{\alpha=1}^{n(\mathbf{u})} \nu_\alpha^{PK}(\mathbf{u}; z_k)\, X(\mathbf{u}_\alpha)\end{aligned}$$

To account for scaling differences between the original data values and the indictor transformation, probability kriging replaces the original data with their standardized ranks (Goovearts, 1997). The inclusion of data ranks allows the estimator to differentiate samples with similar indicator transformation values (Goovaerts, 1997).

Each kriging method was run using the Geostatistical Analyst tool in ArcGIS Pro. For each respective method, the threshold value was set to 450-ppm to represent the PA DEP Statewide Health Standard. Variogram models were fit using a lag size of 150 ft and 12 lags total. Gaussian models were selected for all variogram models. Remaining parameters were kept as the defaults for both methods. For each model output, the probability surface and error surface were exported using a mask that removed the non-sampled portions of the study area.

The study area was also broken into sections (i.e., strata) to better reflect the sampling scheme used to collect data and in consideration of the uneven distribution of the samples. Samples were collected in different regions over the course of several years, resulting in varying sampling patterns across the site. Three sections were chosen, referred to as the “northern”, “southern”, and “western” sections (Figure 4). Figure 5 illustrates box plots created based on the original sampled lead levels for all three sections, showing a clear difference in the range of lead values across the different areas on site.

Both indicator and probability kriging were re-run for each defined section; i.e., northern, western and southern sections of the study area. Individual semivariogram models were fit using only the samples located within the respective section. This allowed each semivariogram model to be fine-tuned using a smaller subset of the data to better reflect the sampling pattern and spatial structure of lead levels within the individual sections. Most kriging parameters were set to the same values used when kriging across the entire site; e.g., indicator variables used a threshold of 450-ppm and all variograms used a Gaussian model. Changes were made, however, to the lag distances used to estimate the semivariograms models to better capture the spatial structure within the individual sections. The northern and southern sections had a lag size of 100 ft with 12 total lags, while the western section had a lag size of 100 ft with 10 total lags. As with the outputs for the whole site, a probability and error surface were exported using a mask.

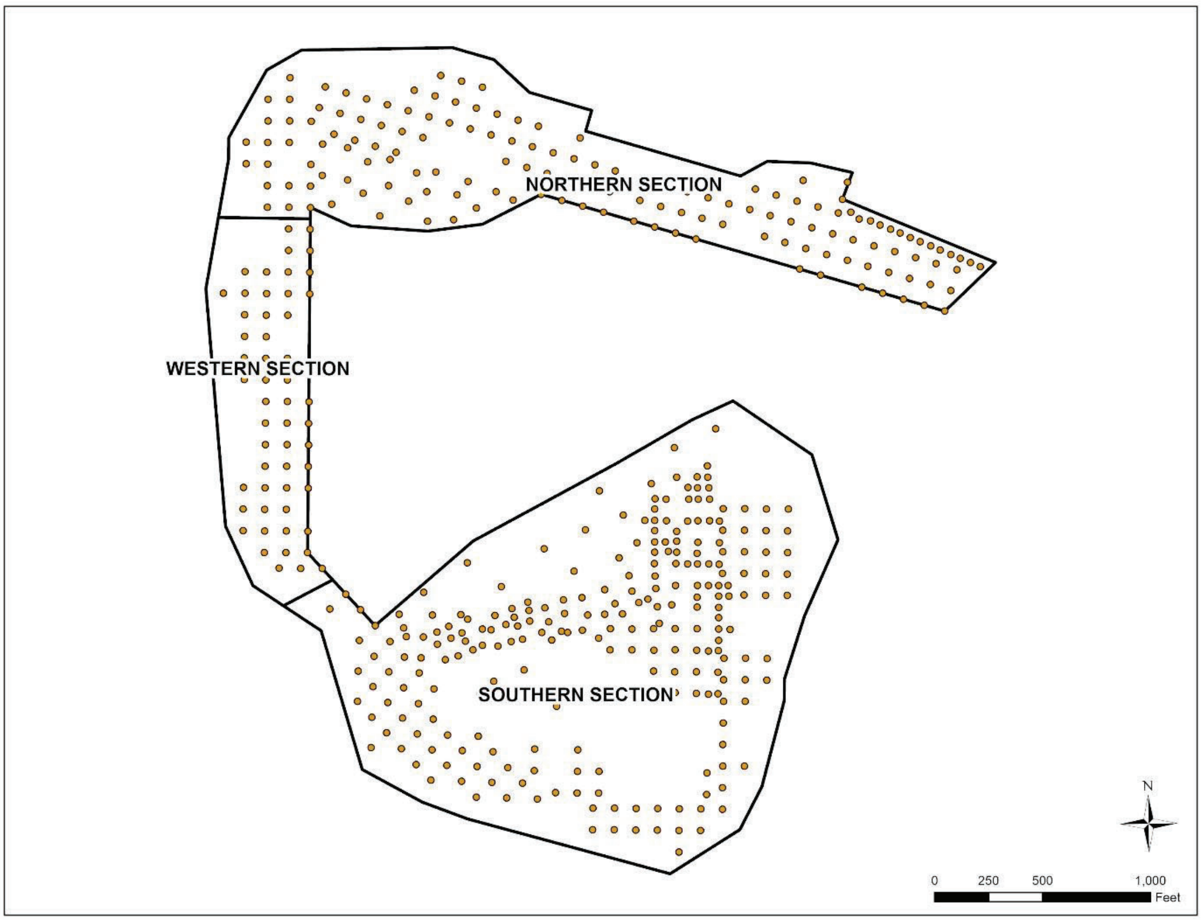

Figure 4: Sectioned areas.

Figure 5: Box plots showing the distribution of data for the sectioned areas.

Results/Discussion

Figure 6 shows the probability surfaces for indicator and probability kriging run for the entire site and individually for each section. The red areas indicate a one hundred percent confidence of exceeding the 450-ppm threshold, while blue indicates a zero percent confidence. At first glance, indicator kriging appears to have done a better job than probability kriging overall when considering the location of sample points that exceeded the 450ppm threshold. One area of the site where this is shown is in the most eastern portion of the northern section, where samples that exceed 450-ppm are shown with a higher confidence and the surrounding areas are shown with lower. The probability kriging outputs do not show this differentiation as clearly. The exception to this trend was the probability surface produced using probability kriging for the western section, which also appears to have done well when considering the underlying point pattern. Both western outputs show low confidence where points are below 450-pmm, and high confidence where they are above.

Figure 7 shows the accompanying error surfaces for these model runs. The green areas indicate the lowest errors, while the red indicate the highest errors. When considering the associated error surfaces, indicator kriging for the sectioned data had the lowest overall error and was moderately successful in predicting locations that exceeded the established threshold particularly in the northern and western sections. When considering kriging performance for individual sections, probability kriging conducted in the western section displayed the lowest errors.

Confidence interval thresholds were created by contouring the probability surfaces to extract the desired values. This analysis was only performed on the kriging probability surfaces created using the sectioned data as these probability surfaces produced the best results. Figure 8 shows extracted confidence intervals, where the purple contours represent a 95 percent confidence in that line being the 450-ppm contour and the pink contours represent a 75 percent confidence. These threshold confidence lines show again that indicator kriging performed best for the northern and southern sections, and performed well for the western section. But that probability kriging did the best for the western section. The indicator kriging thresholds for the northern and southern sections show almost every point above 450-ppm within the 95 percent area, and all the points for the 75 percent area. The western section for indicator kriging did not encapsulate all the points above 450-ppm for the 95 percent area but did for 75 percent. But probability kriging did show all these points within the 95 and 75 percent areas. Table 1 shows a comparison of delineated areas for each method and the chosen confidence intervals. This shows the large variations in the predicted surfaces, with the total area differing by over 1,000,000 square feet for the total area for 95 percent. The western sections showed the least variation between methods, with the differences between both confidence intervals only totaling around 10,000 square feet.

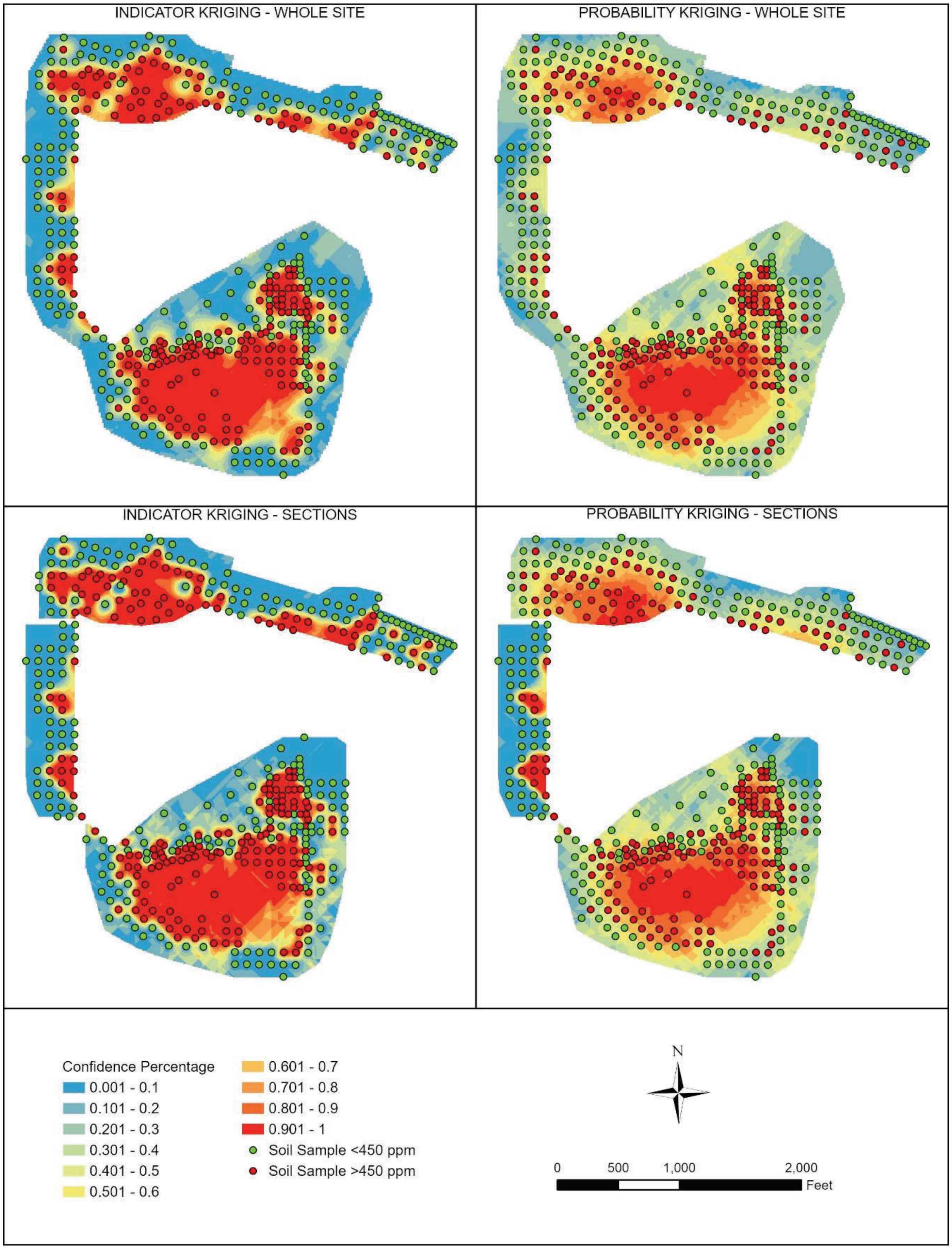

Figure 6: Probability surfaces for whole site and sectioned site for probability and indicator kriging.

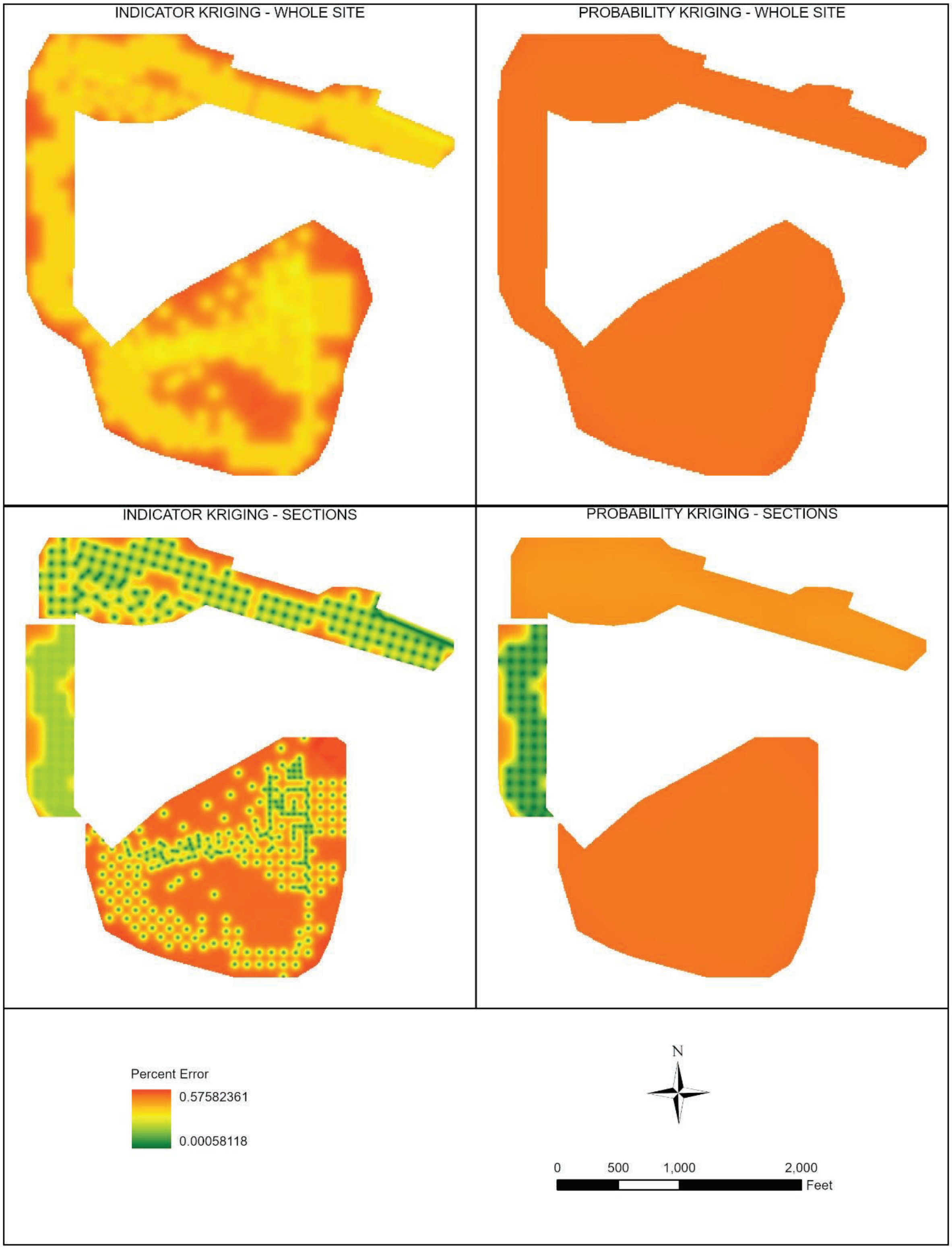

Figure 7: Accompanying error surfaces for the probability surfaces shown on Figure 6.

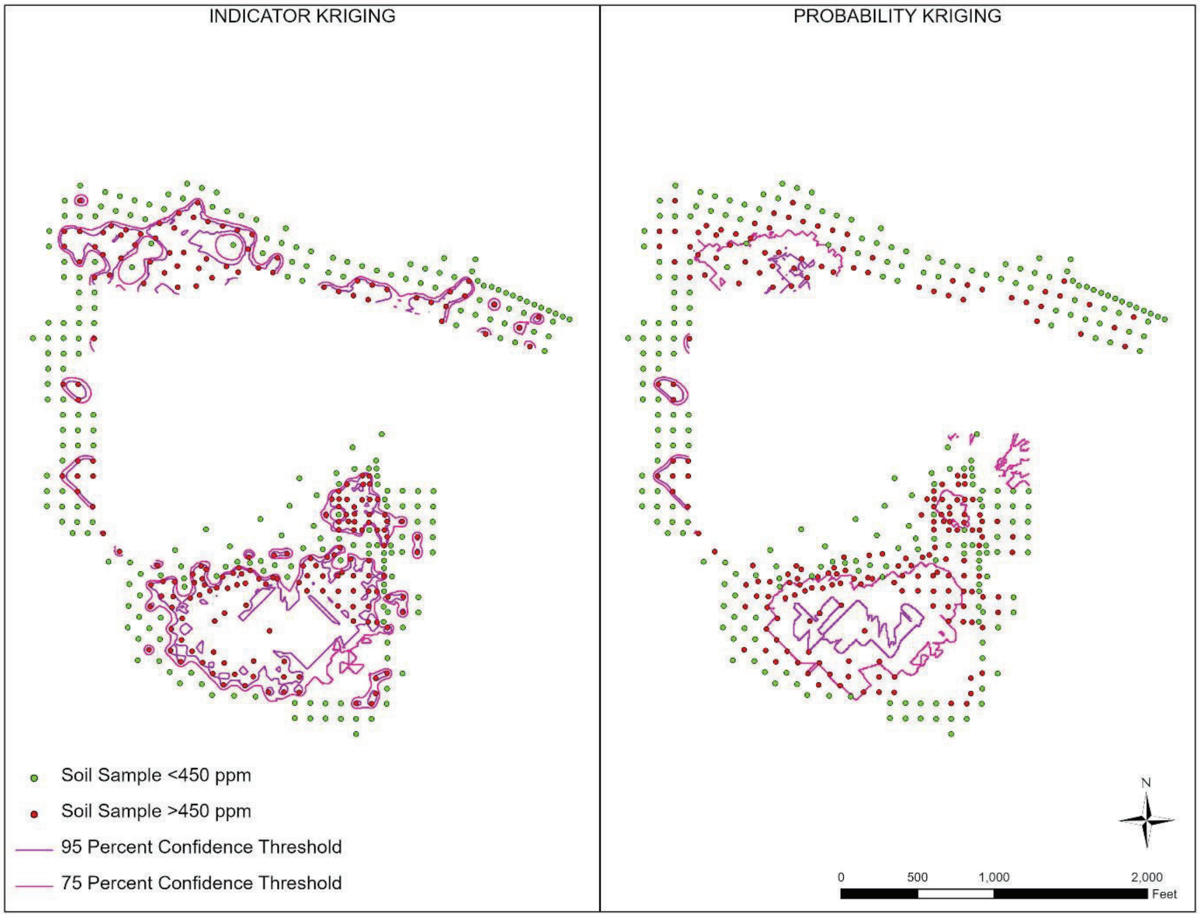

Figure 8: Confidence threshold contours for sectioned data for indicator and probability kriging.

Table 1: Total area of delineated areas for the sectioned data for each method.

Method	95 % - Area (sq. ft.)	75 % - Area (sq. ft.)
Indicator - Total	1,269,106	1,815,567
Probability - Total	236,698	1,111,321
Indicator - north	399,763	579,964
Probability - north	31,890	276,799
Indicator - west	42,536	68,132
Probability - west	53,525	75,740
Indicator - south	826,572	1,167,471
Probability - south	151,283	758,579

Table 2 shows error statistics summarized for each error surface. RMSE represents the root mean square error calculated by measuring the difference between the predicted values and the actual values of the sample points. This is calculated using the following equation:

$$RMSE = \sqrt{\sum_{i=1}^{n} \frac{(\hat{y}_i - y_i)^2}{n}}$$

The minimum, maximum and mean error values were determined by summarizing the resulting error surface; e.g., mean error represents average error predicted for all grid cells within the masked study area extent. This reflects the entire surface as a whole, in comparison to RMSE, which only uses the sample points. Mean errors were lowest for all indicator kriging models when compared to probability kriging models with the exception of the western section, confirming visual observations based on the error surfaces. The lowest mean errors corresponded to the sectioning of the dataset, with higher gains in accuracy observed for indicator kriging in northern section (mean = 0.25637) and probability kriging in the western section (mean = 0.17617). The lowest minimum errors were observed for kriging conducted on the sectioned data as well, with a minimum error value of 0.00058 for indicator kriging in the northern section, 0.00532 for the indicator kriging in the southern section, and 0.01956 for the probability kriging in the western section.

While these error value minimums suggest that accurately estimating the probability of exceeding the lead level threshold is possible, error value means and maximums illustrate that there were locations within the study area that were estimated poorly even when sectioning the data; for example, the southern section had mean and maximum error values greater than 0.4 across all kriging models. One explanation for these high error values is the sampling pattern used to obtain lead level estimates. In the southern region, sample selection resulted in a gap at the center of the section. This area lacking sample points was poorly estimated. In addition, it is possible that the spatial structure of the lead values in the sample set alone may not be enough to accurately estimate the contamination on site. It is possible that another key variable could be added to the model to improve the estimation. For example, if specific shooting stands on site were used more than others, this could result in proportionally more lead landing in the shot cone of those stands. The challenge is obtaining this data, if applicable, and correctly incorporating the data into the kriging method provided that a secondary relationship even exists.

Table 2: Summary of error statistics

Output	Point RMSE	Grid Error - Min	Grid Error - Max	Grid Error - Mean
Indicator - whole site	0.42051	0.31992	0.55629	0.40820
Probability - whole site	0.43416	0.50965	0.52164	0.51150
Indicator - north	0.43044	0.00058	0.53857	0.25637
Probability - north	0.43498	0.46300	0.48823	0.46835
Indicator - west	0.38162	0.18185	0.51049	0.25601
Probability - west	0.40656	0.01956	0.51440	0.17617
Indicator - south	0.44083	0.00532	0.57582	0.41865
Probability - south	0.42702	0.50679	0.51872	0.50913

Indicator kriging generally performing better than probability kriging was not an expected result, as previously cited research found estimation improvements when employing probability kriging (Juang and Lee (2000); Adhikary et. al. (2010). One possible explanation for the improved performance of indicator kriging as demonstrated in this study is that the range of sampled lead levels for this site is much larger than for either of those studies. This study had a range of 7.7 to 346,000-ppm, while the Juang and Lee study's range for lead was 9.52 to 126.67. It appears that the binary nature of indicator kriging lessened the impact of the extreme outliers. The typical downside of indicator kriging is the loss of information when applying the indicator transformation, but it appears that this may have been a benefit in this case. The results in the western section, which saw improved performance for probability kriging, appear to support this convention. The western section had a much smaller range in lead level values compared to the northern and southern sections. The maximum lead level measured was 11,100-ppm, compared to 346,000-ppm and 203,000-ppm for the southern and northern sections respectively. The western section also had a more even sampling distribution; although the impact of the sampling distribution on kriging results needs further exploration.

Spatial interpolation based on a limited number of samples will never be a perfect representation of contamination across a site. And certainly, an interpolation is only as good as the data it is fed. If uneven sample distributions can be avoided when sampling plans are being made, estimations can be improved.

It is also critical that sampling procedures honor established sampling protocols to ensure confidence in the measured lead levels. For this site, it is very likely that lead shot was in some of the earlier samples resulting in extreme skewing and outlying observations in the lead level distribution. Despite these acknowledged challenges, this study demonstrated that indicator and probability kriging can be successfully employed to estimate the probability of exceeding an established lead level threshold. Further, the creation of a probability surface in both kriging methods offers flexibility in delineating soil contamination as it allows a remediator to select a confidence level in line with the perceived risk determined by their client.

Conclusion

This study demonstrated that probability kriging and indicator kriging can produce reasonable estimates of lead soil contamination for the shooting range examined in this study. Indicator kriging, in general, outperformed probability kriging, possibly owing to the extremely skewed distribution of lead levels in the measured sample points. Sectioning the site into strata also resulted in improved estimations, as sectioning allowed the kriging model to account for differences in the spatial structure of lead levels across the site. Moving forward, care should be taken when planning sample locations to ensure they are as evenly distributed as the site will allow. But when this is not possible, the results reveal that indicator kriging may help delineate remediation areas where probability kriging fails.

References

Adhikary, Partha Pratim, Ch. Jyotiprava Dash, Renukabala Bej, and H. Chandrasekharan. “Indicator and Probability Kriging Methods for Delineating Cu, Fe, and Mn Contamination in Groundwater of Najafgarh Block, Delhi, India.” *Environmental Monitoring and Assessment* 176, no. 1 (August 5, 2010): 663–76. https://doi.org/10.1007/s10661-010-1611-4.

Alexander, Shanna. “Lead Contamination in Soil (ArcGIS).” *Geospatial Analysis for Optimization at Environmental Sites* GRO-1 (2016). https://gro-1.itrcweb.org/lead-contamination-in-soil-arcgis/.

“Best Management Practices for Lead at Outdoor Shooting Ranges.” Overviews and Factsheets. US EPA, June 2005. https://www.epa.gov/lead/best-management-practices-lead-outdoor-shooting-ranges.

Brus, Dick J., and Gerard B. M. Heuvelink. “Optimization of Sample Patterns for Universal Kriging of Environmental Variables.” *Geoderma* 138, no. 1 (February 15, 2007): 86–95. https://doi.org/10.1016/j.geoderma.2006.10.016.

“Clay Pigeon Shooting Basic Guide .” Adventure Sports. Accessed March 26, 2023. https://www.adventuresport.co.uk/blog/clay-pigeon-shooting-basics.

Dahlem, Matt. “Environmental Remediation Costs: Estimating and Funding Cleanup.” Fehr Graham. Accessed March 22, 2023. https://www.fehrgraham.com/about-us/blog/environmental-remediation-costs-estimating-and-funding-cleanup-fg.

De Smith, Michael, Goodchild, Michael F., and Longley, Paul A. Geospatial Analysis: A Comprehensive Guide to Principles, Techniques and Software Tools, 6th Ed. https://www.spatialanalysisonline.com/, 2021.

Department of Environmental Protection. “Statewide Health Standards,” November 20, 2021. https://www.dep.pa.gov:443/Business/Land/LandRecycling/Standards-Guidance-Procedures/Pages/Statewide-Health-Standards.aspx.

Dobrescu, Andreea-Iulia, Agnes Ebenberger, Julia Harlfinger, Ursula Griebler, Irma Klerings, Barbara Nußbaumer-Streit, Andrea Chapman, Lisa Affengruber, and Gerald Gartlehner. “Effectiveness of Interventions for the Remediation of Lead-Contaminated Soil to Prevent or Reduce Lead Exposure - A Systematic Review.” *Science of The Total Environment* 806 (February 1, 2022): 150480. https://doi.org/10.1016/j.scitotenv.2021.150480.

Francos, Nicolas, Asa Gholizadeh, and Eyal Ben Dor. “Spatial Distribution of Lead (Pb) in Soil: A Case Study in a Contaminated Area of the Czech Republic.” *Geomatics, Natural Hazards and Risk* 13, no. 1 (December 31, 2022): 610–20. https://doi.org/10.1080/19475705.2022.2039786.

GIS Resources. “Classification of Interpolation,” October 23, 2013. https://www.gisresources.com/classification-of-interpolation_2/.

GISGeography. “Kriging Interpolation - The Prediction Is Strong in This One.” GIS Geography, February 4, 2017. https://gisgeography.com/kriging-interpolation-prediction/.

Goovaerts, Pierre. *Geostatistics for Natural Resources Evaluation*. Oxford University Press, 1997.

Griffith, Daniel A. “The Geographic Distribution of Soil Lead Concentration: Description and Concerns.” *Journal of the Urban and Regional Information Systems Association* 14, no. 1 (2002): 5–16.

Hardison, Donald W., Lena Q. Ma, Thomas Luongo, and Willie G. Harris. “Lead Contamination in Shooting Range Soils from Abrasion of Lead Bullets and Subsequent Weathering.” *The Science of the Total Environment* 328, no. 1–3 (July 26, 2004): 175–83. https://doi.org/10.1016/j.scitotenv.2003.12.013.

Juang, Kai-Wei, and Dar-Yuan Lee. “Comparison of Three Nonparametric Kriging Methods for Delineating Heavy-Metal Contaminated Soils.” *Journal of Environmental Quality* 29, no. 1 (January 2000): 197–205. https://doi.org/10.2134/jeq2000.00472425002900010025x.

“Lead | ToxFAQs™ .” ATSDR, August 7, 2020. https://wwwn.cdc.gov/TSP/ToxFAQs/ToxFAQsDetails.aspx?faqid=93&toxid=22.

"Lead in Soil." U.S. Environmental Protection Agency (US EPA), August 2020. https://www.epa.gov/sites/default/files/2020-10/documents/lead-in-soil-aug2020.pdf.

Liu, Yaolin, Yiyun Chen, Zihao Wu, Bozhi Wang, and Shaochen Wang. "Geographical Detector-Based Stratified Regression Kriging Strategy for Mapping Soil Organic Carbon with High Spatial Heterogeneity." *CATENA* 196 (January 1, 2021): 104953. https://doi.org/10.1016/j.catena.2020.104953.

Miryousefiaval, Zahra, Abbasali Zamani, and Younes Khosravi. "Comparison of the Interpolation of Lead and Zinc Accumulation in the Soils around Zanjan Lead and Zinc Corporation Using Laboratory and Landsat Data." *Journal of Human Environment and Health Promotion* 6, no. 4 (December 10, 2020): 153–58. https://doi.org/10.29252/jhehp.6.4.1.

O'Sullivan, David, and David J. Unwin. *Geographic Information Analysis*. Second Edition. John Wiley & Sons P&T, 2010.

Sanderson, Peter, Fangjie Qi, Balaji Seshadri, Ayanka Wijayawardena, and Ravi Naidu. "Contamination, Fate and Management of Metals in Shooting Range Soils—a Review." *Current Pollution Reports* 4, no. 2 (June 1, 2018): 175–87. https://doi.org/10.1007/s40726-018-0089-5.

"The Main Three Types of Environmental Remediation and Reclamation." Anderson Engineering, February 25, 2021. https://www.andersoneng.com/the-main-three-types-of-environmental-remediation-and-reclamation/.

"Understanding Probability Kriging—ArcMap | Documentation." Esri. Accessed April 30, 2024. https://desktop.arcgis.com/en/arcmap/latest/extensions/geostatistical-analyst/understanding-probability-kriging.htm

US EPA, OLEM. "Lead at Superfund Sites: Human Health." Overviews and Factsheets, March 26, 2015. https://www.epa.gov/superfund/lead-superfund-sites-human-health.

"What Is Sporting Clays?" NSCA. Accessed March 26, 2023. https://nsca.nssa-nsca.org/what-is-sporting-clays-2/.